FISEVIER

Contents lists available at ScienceDirect

Biomass and Bioenergy

journal homepage: www.elsevier.com/locate/biombioe



Research paper

Production and characterization of H₂S and PO₄³⁻ carbonaceous adsorbents from anaerobic digested fibers



Michael Ayiania^a, Felix Martin Carbajal-Gamarra^{a,b}, Tsai Garcia-Perez^c, Craig Frear^d, Waled Suliman^a, Manuel Garcia-Perez^{a,*}

- a Department of Biological Systems Engineering, Washington State University, L.J. Smith Hall, 1935 E. Grimes Way, Pullman, WA, 99164-6120, United States
- ^b University of Brasília, Faculty Gama, Brasilia, DF, St. Leste Projeção A Gama Leste, Brasília DF, 72444-240, Brazil
- c Faculty of Chemical Sciences, Universidad de Cuenca, Ecuador
- ^d Regenis, Ferndale, WA, USDA, United States

ARTICLE INFO

Keywords: Anaerobically digested fiber Pyrolysis Biochar Hydrogen sulfide Phosphate

ABSTRACT

Anaerobic digestion (AD) is an important technology to produce biogas from dairy manure. Although the AD of dairy manure results in the harnessing of the energy contained in manure, most of the nutrients (phosphorous and nitrogen) remain in the liquid effluent, representing an important source of pollution. Additionally, the biogas produced contains H_2S and CO_2 , limiting its practical use as fuel. In this paper, we report the production and use of a carbonaceous adsorbent from AD fibers for the removal of hydrogen sulfide (H_2S) from biogas and phosphate (PO_4^{3-}) from aqueous liquid effluents. The adsorbents studied were produced via slow pyrolysis between 350 and 800 °C followed by CO_2 activation. The elemental and proximate analyses, surface area and pore size distribution of each of the adsorbents studied are reported. Their adsorption capacities were assessed using H_2S breakthrough and PO_4^{3-} batch equilibrium tests. The sorption capacity varied between 21.9 and 51.2 mg g⁻¹ for H_2S and between 4.9 mg g⁻¹ and 37.4 mg g⁻¹ for PO_4^{3-} . Commercially available activated carbon studied adsorbed 23.1 mg g⁻¹ H_2S and 15.7 mg g⁻¹ PO_4^{3-} . The results show that the retention of H_2S and PO_4^{3-} compounds were governed by the ash content, surface area and pH. Adsorption mechanisms for H_2S and PO_4^{3-} sorption are proposed.

1. Introduction

Anaerobic Digestion (AD) is a technology that converts organic wastes (e.g., dairy farm manure) into methane [1]. The process relies on a complex mixture of symbiotic microorganisms [2,3]. Odor reduction and pathogen control are other benefits of AD [4]; however, this process also has its drawbacks associated with high hydrogen sulfide (H₂S) concentrations in the resulting biogas and high content of nutrients (phosphorous (P) and nitrogen (N)) in its liquid effluent [5–10]. High H₂S concentrations limit biogas use for internal combustion engines [11], and the presence of P and N in the liquid effluent is an important source of water pollution [12,13].

While numerous chemical, physical and biological methods exist for separation and removal of phosphorus from AD effluents and $\rm H_2S$ from biogas [14–16], many of the solutions are problematic from a cost prospective, particularly with respect to annual operating and maintenance expenses [17]. Correspondingly, academic research continues with respect to treatment approaches that can minimize cost concerns,

preferably through integrated solutions utilizing internal co-products from the AD process.

Academic literature shows a wealth of char-related research related to nutrient removal from liquid digestates [5,13,18-21], and H₂S from biogas [21,22] using biochars. Sethupathi et al. [21] studied the adsorption of CH₄, H₂S and CO₂ in biochars produced from four lignocellulosic feedstocks (perilla, soybean stover, Korean oak and Japanese oak). The authors [21] observed poor adsorption of CH₄ compared with H₂S and CO₂ and competition for adsorption sites. Based on these results they suggested that biochar could be a promising material for biogas purification. Guo et al. [5] developed and characterized physically and chemically activated carbons from oil palm shell for H2S removal. The chemically activated carbon had better performance. Sun et al. [19] studied H2S adsorption in a biochar produced in a fluidized bed reactor at 450 °C. The authors obtained a biochar with specific surface area of 60 m² g⁻¹ and with a maximum sulfur removal capacity of 70 mg g^{-1} [19]. Two other groups [22,23] studied in great detail the use of activated carbons (AC) for H₂S removal. In 2001 [24], the

^{*} Corresponding author. Department of Biological Systems Engineering, LJ Smith 205, PO Box 646120, Pullman, WA, 99164-6120, United States. E-mail address: mgarcia-perez@wsu.edu (M. Garcia-Perez).

authors reported the production of carbonaceous H2S adsorbents from sewage sludge-derived materials. The resulting material has an H₂S adsorption capacity twice of those obtained from coconut shell [24] The authors attributed this high adsorption by the presence of iron, zinc and copper. A year later the same group [22] studied the role of NaOH in H₂S adsorption and found that by increasing the pH, NaOH causes an increase in the HS⁻ ion concentration, which can then be further oxidized to elemental sulfur. In 2005, Bagreev & Bandosz [25] studied the use of five new carbonaceous adsorbents on H₂S adsorption. They found that depending on the pH of the condensed water on the carbon surface, H₂S could be oxidized into elemental sulfur or sulfuric acid [25]. The presence of high volumes of micropores was very important. The catalytic centers identified were nitrogen-containing basic groups and metals (iron and alkali and alkaline earth) [25]. Several techno-economic analyses have been reported in the literature of anaerobic digestion systems with H₂S removal using activated carbon [26,27]. In their analysis Pipatmanomai et al. [27] used an average activated carbon H₂S adsorption capacity of 62 mg H₂S/g carbon.

Several exotic biomass feedstocks (orange waste gel, sugar beet, tomato tissues) have been used to produce phosphate removal adsorbents [28,29]. A zirconium (IV) immobilized biochar was developed and characterized by Biswas et al. [29]. At pH 9 more than 85% phosphate removal was achieved, resulting in a biochar with 57 mg-P g⁻¹. Yao et al. [20] studied the use of anaerobically digested sugar beet tailings for phosphate removal from an aqueous solution. The authors [20] found the resulting biochar to be an excellent phosphate adsorbent. Two years later Yao et al. [28] published a paper on the mechanism of phosphate removal on biochars produced from Mg-enriched tomato tissues. The maximum phosphate sorption capacity obtained was $100\,\mathrm{mg\,g}^{-1}$ [28]. An activated carbon developed from coir pith was studied by Kumar at al [30], and a maximum removal capacity was observed at pHs between 6 and 10. Namosivayam and Sangeetha [31] produced a ZnCl2 chemically-activated carbon from coir pith for phosphate removal. A biochar with a capacity to adsorb 5.1 mg g^{-1} was obtained. Maximum adsorption capacity was found at pHs between 3 and 10. Zhang et al. [32] synthesized porous MgO-biochar nanocomposites for removal of phosphate and nitrate from aqueous solutions from sugar beet tailings and peanut shells. The resulting material showed excellent removal capacities as high as $835\,\mathrm{mg\,g^{-1}}$ for phosphate.

Because the problems of $\rm H_2S$ removal from biogas and $\rm PO_4^{3^-}$ removal from aqueous effluents are relevant to addressing issues encountered in anaerobic digestion, it is sensible to try to develop carbonaceous adsorbent materials from the AD fibers generated by these systems. AD fiber can be easily separated and dewatered from screens and screw presses, producing a solid with approximately 30% dry matter, but with a still significant ash content [33], suitable for conversion to char [13]. Streubel et al. [34] produced a biochar from AD fibers for phosphorous removal from dairy lagoons with an average of 381 mg $\rm L^{-1}P$ removal. The carbonaceous materials herein developed from AD fibers will be used as part of the bio-refinery concept shown in the graphical abstract. Because sulfur and phosphorous are plant nutrients, the carbonaceous materials loaded with these compounds can be commercialized as fertilizers [18,20,35–37].

Despite several papers on the use of biochar from lignocellulosic materials as adsorbent for $\rm H_2S$ and $\rm PO_4^{\ 3-}$, we were unable to find information on the production of activated carbons from AD dairy fibers for the removal of these two pollutants. Building upon the previous work on char-related co-products for phosphorus and $\rm H_2S$ control, the aim of this research was to convert AD fiber to activated carbon at different temperatures (350–800 °C) and to evaluate the resulting carbonaceous adsorbents for their capacity to adsorb phosphorus and $\rm H_2S$.

2. Materials and methods

2.1. Anaerobic digested fiber collection

Anaerobically digested dairy fiber was collected from George DeRuyter and Sons Dairy Farm in Outlook, WA. This dairy farm uses a flush handling system, where the dilute manure wastewater is sent to a clarifier before entering a mesophilic, 20-day mixed plug flow anaerobic digester. After digestion, the effluent is sent to a slope screen attached to a dewatering roller, which presses the effluent for mechanical recovery of digested fibrous solids with an approximate moisture content of 72 wt%. A representative portion of the digested fiber was transferred to Washington State University (WSU), where it was partially dried at ambient conditions for one week. The AD fiber was subsequently dried at 103 °C for 24 h as described elsewhere [38]. The commercial activated carbon used to compare the performance of our biochar was obtained from Cabot Norit Activated Carbon Americas Inc (Boston, MA).

2.2. Production of biochar and physical activation

A series of biochars were obtained by slow pyrolysis and activation with CO₂ at temperatures between 350 °C and 800 °C from AD fiber in a Quartz Tube tube furnace reactor of 50 OD x 44 ID \times 1000 L, mm (2"Dx40" L) as shown in Fig. 1. In this research we used a particle size of approximately 1 mm. Briefly, the about \sim 5 g sample was kept in contact with N₂ inside the furnace for 30 min at 25 °C. After that, the temperature was increased from 25 °C to the expected final temperature (350–800 °C) at a heating rate of 10 °C per minute. The sample was kept at the final temperature for 2 h. In the first hour the sample was kept under nitrogen. The sample was then exposed to CO₂ for another hour. Flow rates of 500 mL min $^{-1}$ and 1000 mL min $^{-1}$ for N₂ and CO₂ respectively were employed. Samples were then cooled to temperatures below 25 °C under nitrogen gas before exposure to air. The activated biochar obtained was characterized and used for the adsorption studies.

2.3. ADF and products characterization

Proximate analysis: Proximate analysis was carried out to determine the moisture content, fixed carbon, volatiles, and ash content of the biochars. This test was done using a thermogravimetric analyzer (TGA) SDTA851e (Mettler Toledo, US). Briefly, moisture content was determined as the weight loss after the char was heated in a crucible to 120 °C and held at this temperature for 3 min under nitrogen. Volatile matter was determined as the weight loss after the char was heated to 950 °C (under nitrogen) and held for 5 min and later cooled down to 450 °C. Ash was defined as the remaining mass after the char was subsequently heated to 600 °C and held for 8 min under oxygen flow.

Elemental analysis: Elemental analysis was performed using a TRUSPEC-CHN® (LECO, US) elemental analyzer [38]. Briefly, 0.15 g of samples of biochar were used to determine total carbon (C), nitrogen (N) and hydrogen (H). The oxygen (O) mass fraction was determined by difference (the ash content was taken into account for this calculation).

pH: pH analysis was done following the method described elsewhere [39]. A 0.4 g biochar sample was added to 20 mL DI water. The suspension was shaken with a mechanical shaker at 40 rpm for 1 h and equilibrated for 5 min before measuring the pH with a pH meter (Fisher Scientific Accumet basic AB15).

Gas physisorption analysis for biochar surface area and porosity: Carbon dioxide (CO_2) adsorption isotherms were measured at 273 K on micromeritics TriStar II PLUS Surface Area and Porosity Analyzer (Norcross, GA, USA). Before each analysis, biochar samples were degassed at 250 °C for 18 h under a vacuum of 0.05–0.1 mbar (the degassing temperature was chosen based on the production temperature of the biochar to avoid sample degradation during preparation). CO_2 adsorption isotherms were measured between the partial pressure range

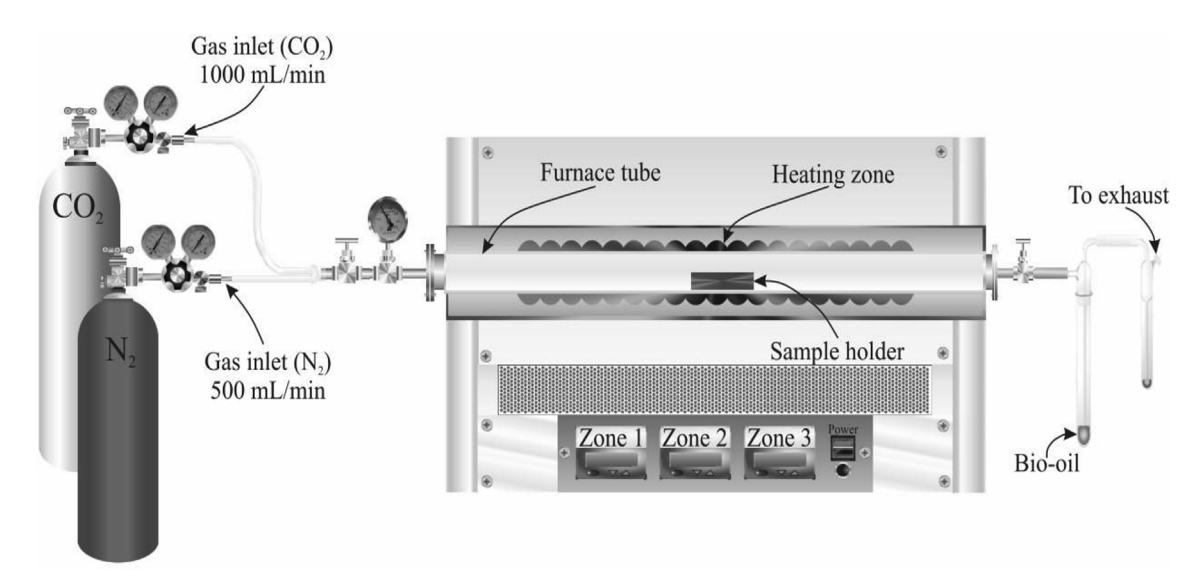


Fig. 1. A scheme of the lab-scale pyrolysis and activation reactor used in this study.

of $p/p^o = 10^{-5}$ to $p/p^o = 0.03$ using 75 set equilibration points. Surface area and micropore volumes were estimated for CO_2 adsorption using the Dubin-Radushkevich (DR) equation [40,41].

Morphological analysis: The biochar surface was visualized by scanning electron microscopy (SEM) using a Hitachi S-570 variable pressure instrument. Biochar samples were analyzed before and after adsorption studies using a magnification range of $200\times$ and 2000x. Due to the conductivity of each sample, no preliminary metal coating was required.

ICP-MS: After biochar production, all the samples were analyzed for the presence of metals. Metal analysis was conducted based on the method described elsewhere [42], in an ICP-MS (Agilent 7500cx) instrument. Samples (~100 mg) were mixed with 3 mL concentrated nitric acid (HNO₃) (69-70%) and 2 mL 30% H₂O₂ in a microwave digester (SP-D, CEM corporation) at 300 °C and 250 psi for 5 min. A 5-min ramp was used to reach digestion conditions. A solution of 1 mL of internal standard was added ($10\,\mu g\,mL^{-1}$, Bi, Li-6, Sc, Tb, and Y) (Accustandard, Inc.) to each digested solution and diluted to 100 mL using Epure water. Operational power was set to 1600 W. Argon carrier gas was set to 0.90 Lmin⁻¹ for the nebulizer and 0.25 Lmin⁻¹ for the makeup. Tuning was performed prior to analysis using a 1 ppb solution of Li⁶ Y, and Ti to achieve sufficient sensitivity over a range of m/z ratios. Calibration was performed using a multi-element standard; all standard solutions and samples included an equal quantity of internal standard. Corrected calibration curves show strong linearity ($R^2 \approx 0.99$) for all elements studied.

2.4. Adsorption studies

 H_2S Adsorption: Fig. 2 is a schematic representation of the experimental set up used. The adsorption tests were carried out in vertically-oriented polycarbonate tubes (6.35 mm internal diameter, 250 mm long). In each experiment, 300 mg of activated biochar was packed in the tube. The tests were conducted at atmospheric pressure and room temperature. A simulated biogas containing 2000 ppm of $\rm H_2S$, 65 vol % $\rm CH_4$, and balance $\rm CO_2$ was used for each adsorption trial. $\rm H_2S$ was then passed through the column of adsorbent at a rate of 10 mL min. $^{-1}$ of gas. The flow rate of gas was controlled by a volumetric flow meter. A 0.1 N HCl solution (500 mL, using domestic water) was employed to humidify the biogas before reaching the column. The concentration of $\rm H_2S$ was monitored using a gas chromatography analyzer (GC; Varian GC3800, equipped with an Agilent CP-SilicaPLOT 50 m \times 0.53 mm x 4 μ m column) with a computer-automated data acquisition program.

The breakthrough concentration was set to be 10% of the initial concentration of $\rm H_2S$. The simulated biogas used for the analyses contained: 0.1995 vol% of $\rm H_2S$, 65.020 vol% of $\rm CH_4$ and 34.78 vol% of $\rm CO_2$. The activated carbon was allowed to reach saturation before the test was stopped.

Batch Equilibrium studies of phosphate adsorption: Biochar samples produced between 350 and 700 °C were tested for capacity to retain PO_4^{3-} . Sodium phosphate buffer (PB) solutions were prepared with nanopure water (> 18 M Ω cm), sodium phosphate monobasic (NaH₂PO₄) and sodium phosphate dibasic (Na₂HPO₄) to guarantee a buffer solution of pH of 7. The concentration range was chosen to represent the nutrient concentration commonly observed in the dairy manure effluents. (0, 10, 30, 50, and 100 mg L⁻¹).

A suspension of 0.2 \pm 0.005 g of activated biochar in 25 mL of PB solution was formed. The mixture was then placed on a horizontal mechanical shaker and left for 24 h in duplicates at each concentration. After shaking, the suspension was allowed to stand for at least 2 h for the particles to settle to the bottom of the tube; the supernatant was later filtered through a 0.45 μm filter paper. The equilibrium concentrations of the filtrates from the adsorption studies were measured by a molybdovanadate method using the acid persulfate digestion method (1.0–100 mgL $^{-1}$) [43]. The experimental results obtained were fitted with the Langmuir isotherm and the Freundlich models. More information on these models can be found elsewhere [44].

3. Results and discussion

3.1. Feedstock and commercial activated carbon characterization

The AD fiber studied yielded 65.4 wt % volatiles, 19.1 wt % fixed carbon and 15.5 wt % ash. It contains 43.1 wt % C, 5.0 wt % H, 2.1 wt % N and 34.3 wt % O (by difference). The compositional results reported for AD fiber are comparable to those found by Sheets et al. [45].

The commercial activated carbon studied yielded 8.9 wt % volatiles, 51.5 wt % fixed carbon, and 40.0 wt % ash. This material contains 54.2 wt % C, 0.7 wt. H, 0.4 wt. N and 1.0 wt % O (by difference). The BET surface determined with nitrogen (Sa $_{\rm N2}$) was 371.8 m 2 g $^{-1}$. A lightly lower surface area was determined with carbon dioxide (Sa $_{\rm CO2}$:290.6 m 2 g $^{-1}$).

3.2. Bio-char characterization

Biochar yield: Table 1 shows the yield of biochar obtained from the

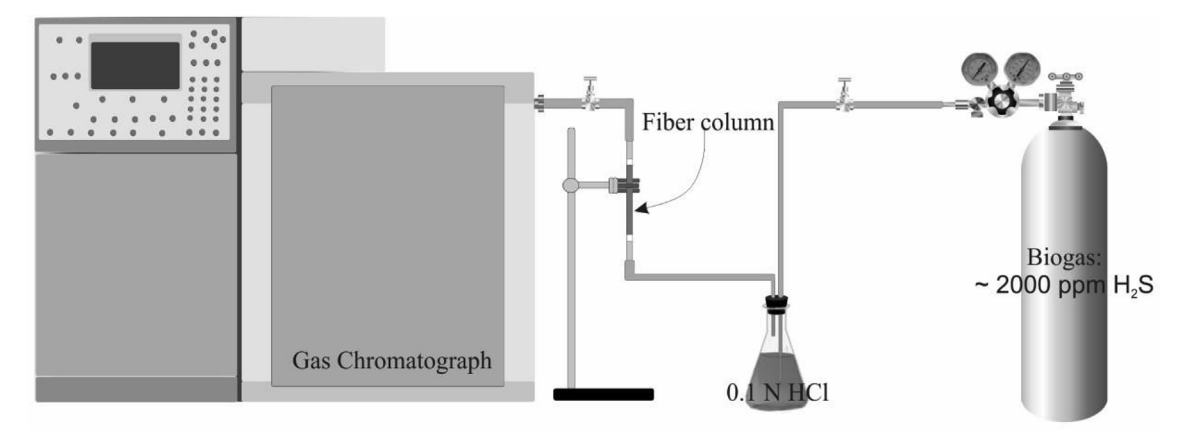


Fig. 2. Schematic of the experimental setup designed to carry out the H₂S breakthrough experiments.

AD fiber. The biochar yield decreased as the production temperature increased from 350 to 800 °C. This trend is attributed to the removal of volatiles by pyrolysis reactions and by the removal of fixed carbon by oxidation with CO2. As the temperature increases crosslinking and aromatization and polymerization reactions take place to form the char. Pyrolysis is responsible for the weight losses at temperatures below 600 °C, and the reduction in char yield over 600 °C is mostly due to char oxidation. The high yields of char observed at 600 °C may be explained by the relatively high content of ash (15.5 wt%) in the AD fiber. The presence of ash is known to catalyze biochar polycondensation and oxidation [46]. Table 1 shows biochar pH increase as a function of production temperature (350-800 °C). This behavior can be explained by the concentration of ash as production temperature increases (see Fig. 3 for trend) [47]. pH values varied from 8.0 to 12.0. This observation is of interest as biochar pH is known to impact both H₂S and phosphate removal [25,48].

Fig. 4 presents the proximate analysis of the resulting biochars produced (ash content, volatile matter and fixed carbon). The ash content in the biochar increases exponentially as production temperature increases. This can be attributed to the accumulation/concentration of the mineral elements during the decomposition of the organic constituents. Meanwhile, the reduction in the fixed carbon at temperatures below 600 °C is mostly due to pyrolysis reactions, and at higher temperatures it is attributed to the activation of the biochar with CO₂. The volatile matter decreased with temperature due to volatilization of organic molecules.

The elemental analysis of each of the carbonaceous products obtained is shown in Fig. 4. The carbon content of the samples remains almost constant till approximately 600 °C. In lignocellulosic materials with low ash content, the carbon content always increases as the pyrolysis temperature increases. The lack of important changes in C content in our samples can be explained by its high ash content. The elemental composition of the volatiles seems to be similar to the elemental composition of fixed carbon plus ash fractions. The carbon content decreases too between 600 and 800 °C due to the oxidation of the fixed carbon to produce CO and $\rm H_2$ [49]. The oxygen content decreases from 19.1 to 5.4 wt% as production temperature increases. The same effect was not observed for nitrogen content, which remained practically constant with increase in temperature for all the biochar samples, this might be attributed to formation of heterocyclic stable nitrogen

functionalities such as pyridines and pyrroles [50]. At 800 °C, however, we observed an important decrease in nitrogen content. The presence of N in carbonaceous materials is known to impact positively some of their catalytic properties [51,52]. The gradual decrease of H/C as temperature increases is an indicator of the gradual increase in the size of condensed polyaromatic ring systems [53–56].

Fig. 5 shows how the pore size evolves as a function of production temperatures. Pore volume grows as the pyrolysis temperature increases from $350\,^{\circ}\text{C}$ to $750\,^{\circ}\text{C}$, but at $800\,^{\circ}\text{C}$ the pore volume drops drastically. This behaviour might be due to the fact that at high temperature, the final product was above $90\,\text{wt}\%$ in ash with very little organic carbon, leading to collapse of the structure.

Fig. 6 shows the results obtained for surface area and pore volume at various temperatures resulting from CO $_2$ adsorption. It is seen that the surface area in the biochar increases from 147 to $305\,\mathrm{m}^2\,\mathrm{g}^{-1}$ at $750\,^\circ\mathrm{C}$. In contrast, the biochar obtained at $800\,^\circ\mathrm{C}$ has a surface area of only $31\,\mathrm{m}^2\,\mathrm{g}^{-1}$. This might be attributed to a structural collapse due to the catalytic effect of the alkali and alkaline earth metals (AAEMS) with increasing temperature [57]. CO $_2$ activation produces highly microporous biochar that greatly enhances the diffusion of CO $_2$ during the activation process, thereby promoting the porosity development through removal of its volatile matter [18,49]. Similarly, the micropore volume increased from $0.06\,\mathrm{cm}^3\,\mathrm{g}^{-1}$ to 0.12 and later decreased dramatically at $800\,^\circ\mathrm{C}$ to $0.01\,\mathrm{cm}^3\,\mathrm{g}^{-1}$ due to the collapse of char structure

The content of Ca, Mg and Fe in chars produced at different temperatures is shown in Fig. 7. It was observed that the metal content increases with the ash content. The higher the ash content, the higher the concentration of the mineral components.

3.3. Adsorption studies

 H_2S adsorption studies: The breakthrough results from a thermoseries of activated carbons derived from AD fibers is shown in Fig. 8. The breakthrough time is the point on the curve where the effluent of the adsorbate reaches its maximum allowable concentration, which often corresponds to the treatment goal. Our results clearly show that the production temperature highly influenced the biochar's capacity for H_2S adsorption. The breakthrough time increased between 500 and 750 °C (surface area: $210 \, \mathrm{m}^2 \, \mathrm{g}^{-1}$ to $305 \, \mathrm{m}^2 \, \mathrm{g}^{-1}$) from 1.0 to 11.0 h,

Table 1
Yield of biochar and pH.

T (°C)	350	400	450	500	550	600	650	700	750	800
Yield (wt. %)	72	67	61	54	48	42	35	30	23	17
pH	8	9	9.95	9.85	9.95	10.30	10.50	11.35	12.0	12.0

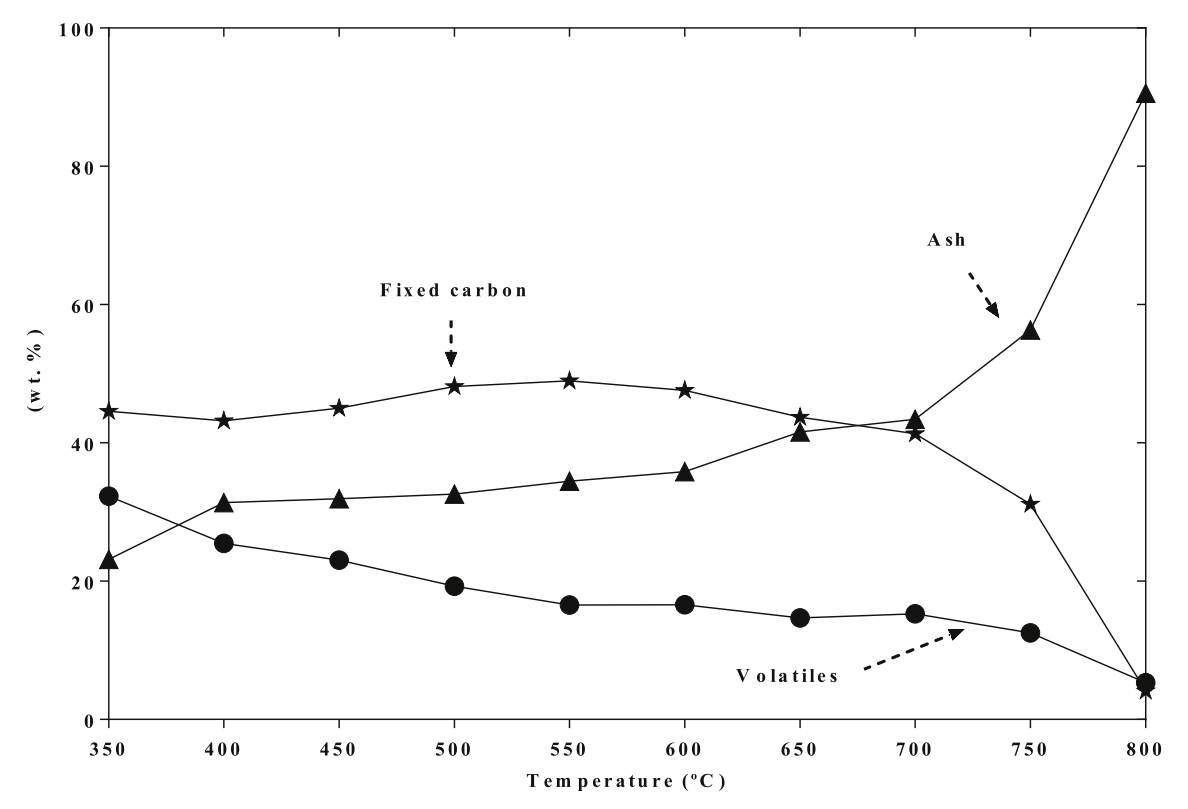


Fig. 3. Ash content, Volatiles, Fixed carbon and moisture content of studied biochar AC350-AC800.

respectively, while the commercial activated carbon took 3.25 h to breakthrough.

The importance of surface area can be appreciated when comparing the performance of the biochar produced at 750 $^{\circ}$ C with that of the biochar produced at 800 $^{\circ}$ C. Adsorption of H₂S is influenced by the presence and speciation of ash and by surface area, pore size and surface chemistry. ICP–MS analysis shows the composition of metals present in the biochar; minerals such as calcium, magnesium, iron, aluminium, and manganese were the most prominent metals found in the

biohars. These metals (except manganese) in previous studies were shown to enhance the adsorption of H_2S [24,25,58,59]. Our results are consistent with a process dominated by two competitive adsorption mechanisms: (1) filling of the micropores and (2) catalytic oxidation of the H_2S to elemental sulfur.

Bagreev and Bandosz et al. [25] reported that for H_2S to be adsorbed it should be oxidized to either elemental sulfur or sulfuric acid, and the extent of oxidation depends on the surface pH of the biochar. Therefore, this process is favorable in basic media, and this study the

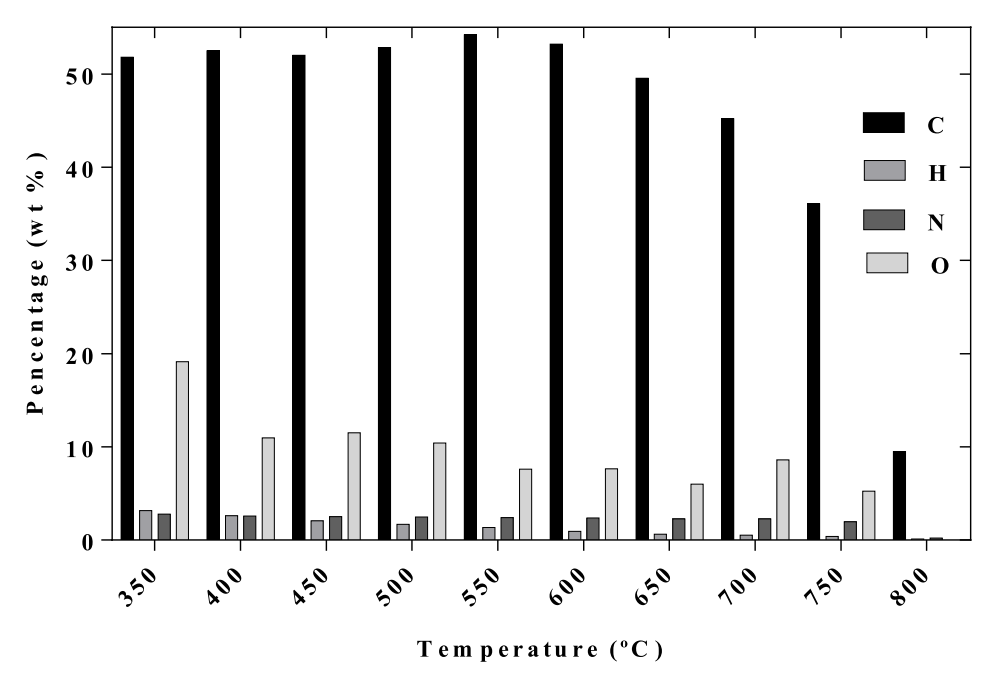


Fig. 4. Elemental composition of biochar produced at different temperatures (350 $^{\circ}$ C -800 $^{\circ}$ C). All percentage values are based on bone dry weight.

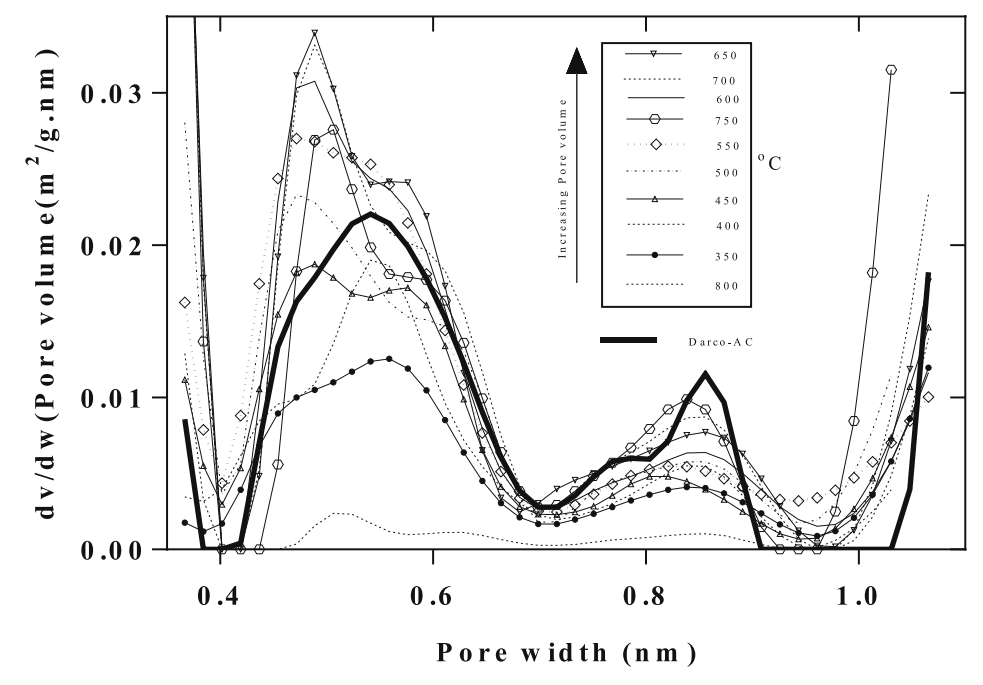


Fig. 5. Pore size distribution of AD fiber biochars.

pH ranged from 8 to 12. The source of alkalinity is attributed to the high inorganic fraction of the biochar–such elevated values of pH makes our biochar alkaline and hence beneficial to $\rm H_2S$ adsorption. Another parameter is the nitrogen content of the biochar, which ranges from 2.8 (wt %) and 2.0 (wt %) for 350 °C–750 °C and 0.2 (wt %) for 800 °C. In the literature [60], it is reported that the presence of nitrogen containing functionalities not only provides basic media, but it also has been proposed to activate oxygen via formation of superoxide ions, which participate in the oxidation of thiolate and $\rm H_2S$ to sulfur and sulfuric acid [60].

Fig. 9 reports the sulfur content of the biochars before and after H₂S

adsorption. Biochars with more than 10 wt% of S were produced. This is very important for the commercialization of this biochar as a source of this nutrient. It is observed that despite the early breakthrough of the biochar at 800 °C relative to biochar at 750 °C, it was able to retain a significant amount of sulfur, hence explaining the participation of the ash in the retention of $\rm H_2S$.

Phosphate adsorption studies: Fig. 10 show the nonlinear isotherm of the adsorption of $PO_4^{\ 3-}$, which clearly depicts an increase in the amount of $PO_4^{\ 3}$ with respect to temperature from 350 °C to 700 °C. Adsorption isotherms were used to describe the relationship between $PO_4^{\ 3-}$ equilibrium concentration and the activated biochar at room

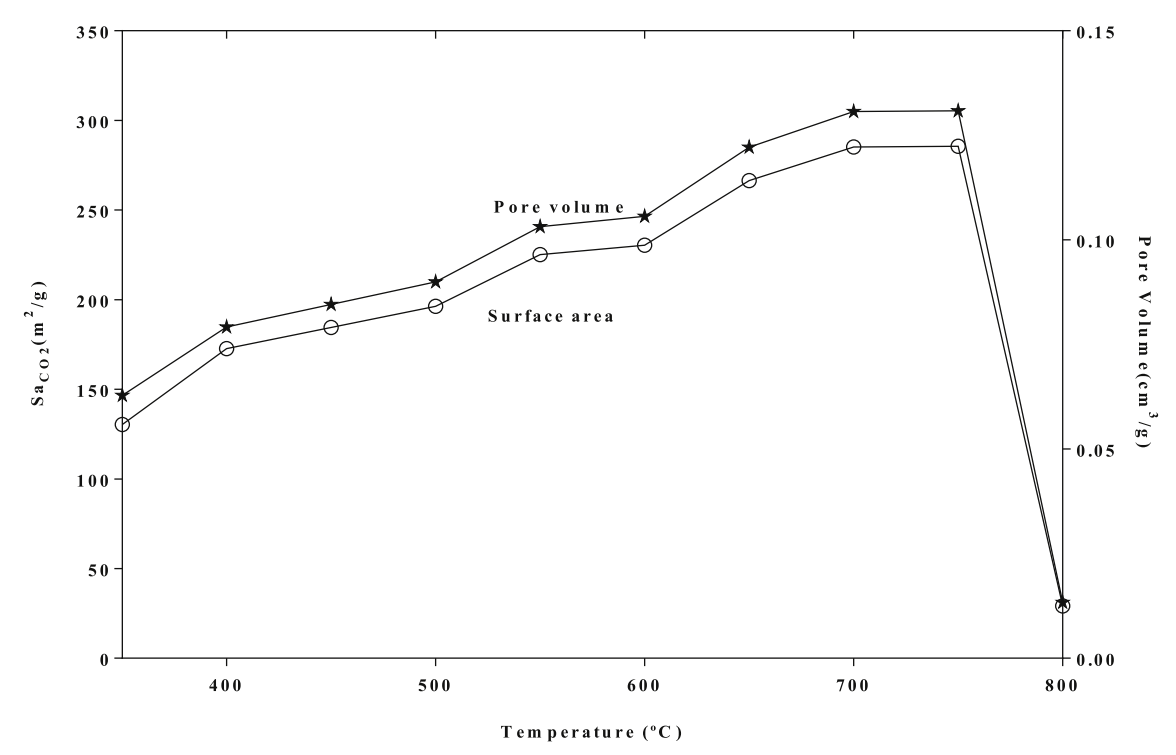


Fig. 6. Surface area and micropore volume of char produced at different temperatures.

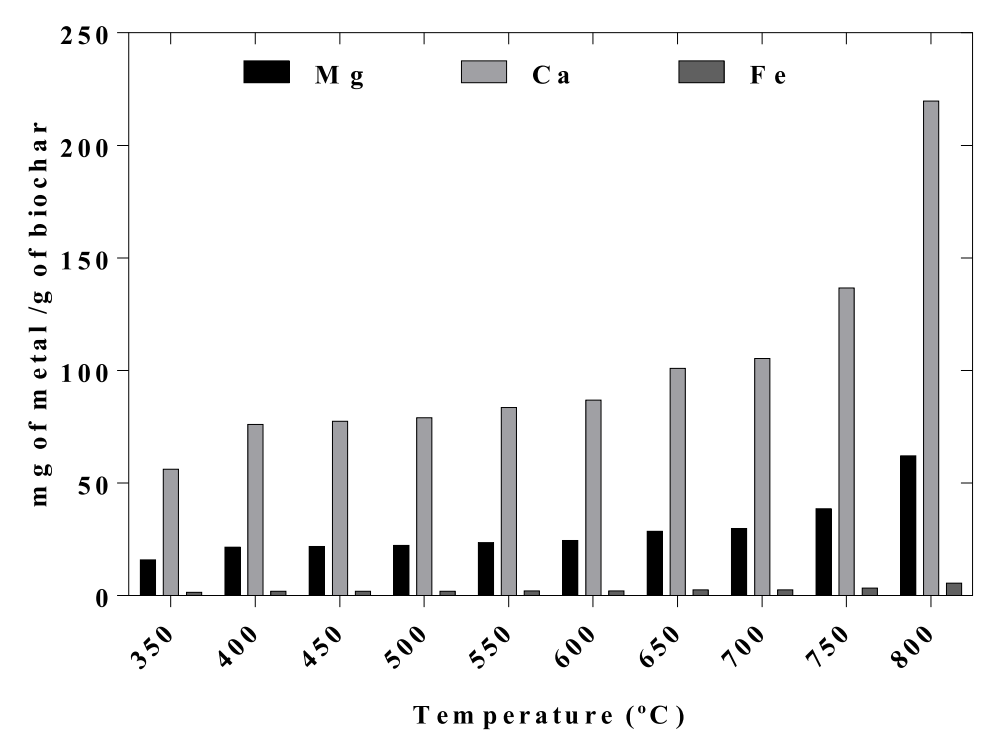


Fig. 7. Mineral content by ICP-MS analysis on AD fiber biochar at different temperatures.

temperature. Fitting the Langmuir model to our experimental data enables qualitative assessment the nature of the adsorption process [[61]].

Table 2 presents the data modeled with both Langmuir and Freundlich models. It is appreciated that the maximum capacity of adsorption is 37.5 mg g^{-1} , obtained for biochar produced at $700 \,^{\circ}\text{C}$. The constant correlation coefficient (R²) and chi-square (χ^2) values of both Langmuir and Freundlich models are presented in Table 3. The R² values of the

Langmuir model (0.918–0.996) were higher than that of the Freundlich model (0.834–0.986). In contrast, the chi-square values of the Langmuir model were significantly lower than the Freundlich model. Therefore, considering these parameters (R^2 and χ^2), we described our data with Langmuir model.

Previous work [62] has identified that the adsorption characteristics of the Langmuir model can be interpreted regarding a dimensionless factor called the separation factor (R_L), such that $R_L = 1/(1 + K_L C_o)$.

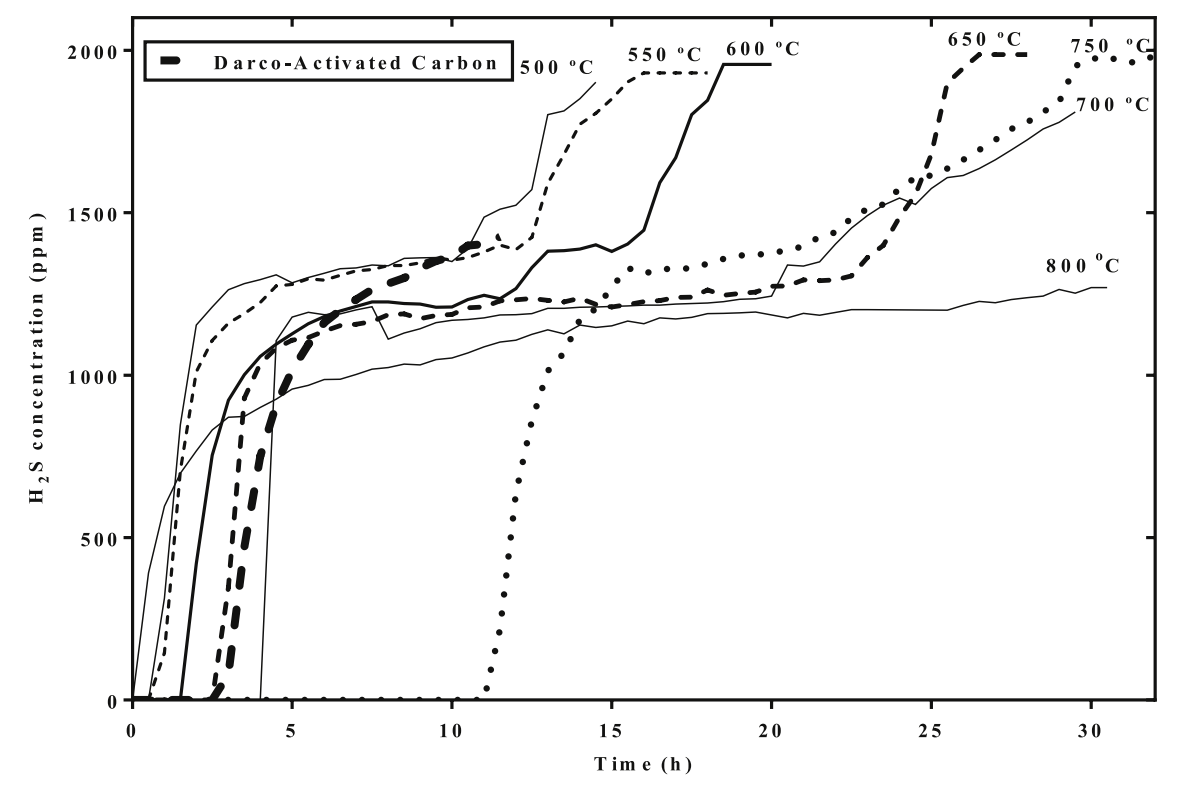


Fig. 8. Breakthrough curves of H₂S on AD biochar pyrolyzed at different temperatures (500°C–800 °C).

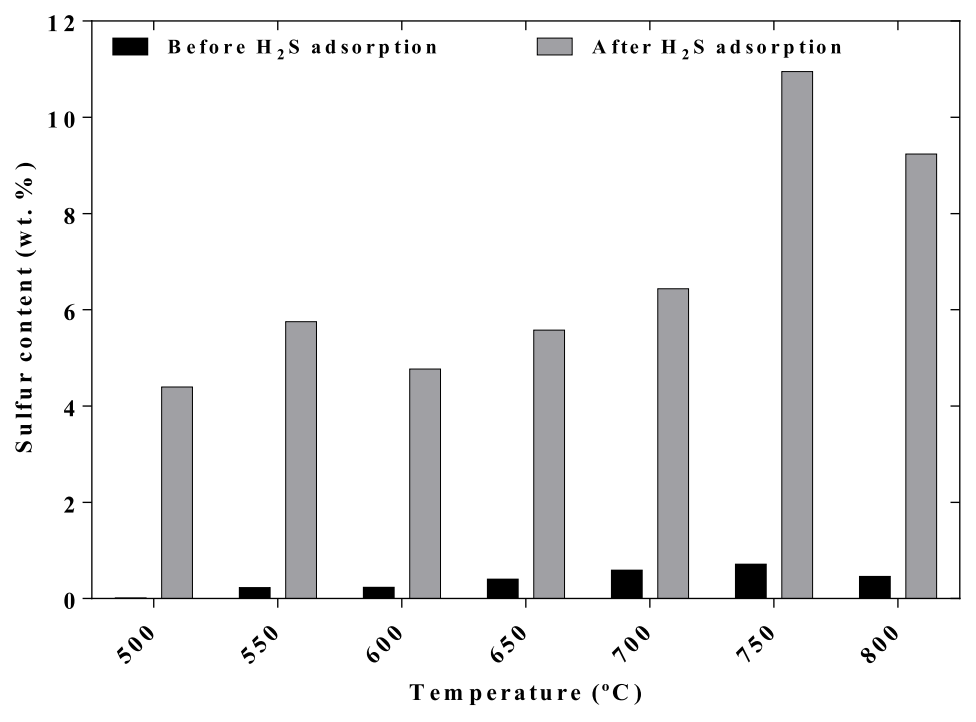


Fig. 9. Sulfur content adsorbed on biochar before and after adsorption of H₂S.

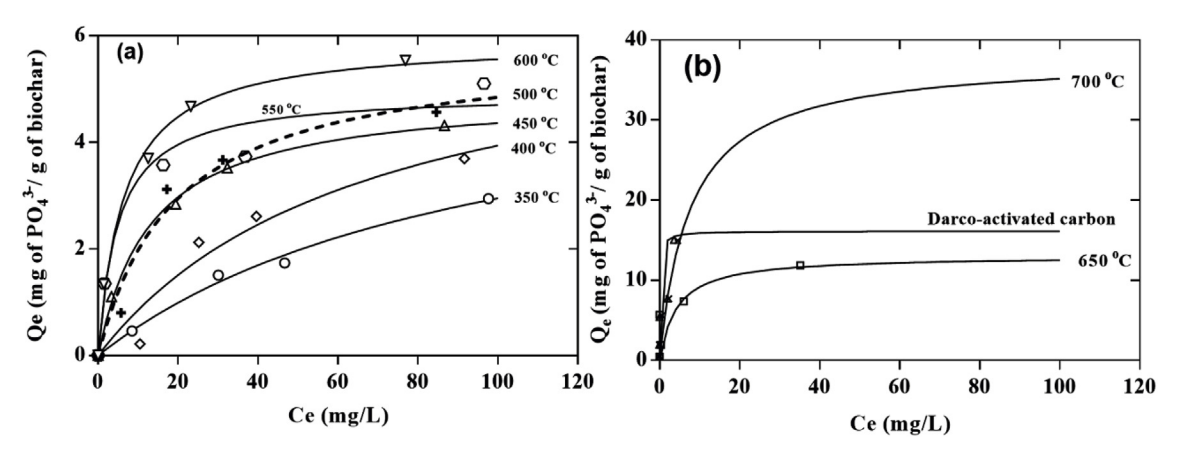


Fig. 10. Adsorption isotherm of PO_4^{3-} from (a) AC350 °C to AC600 °C, (b) from 650 °C, 700 °C and Darco-Activated Carbon. Symbols represent experimental data and lines represent the model.

Table 2 Isotherm parameter of PO_4^{3-} adsorption and deduced parameter from Langmuir and Freundlich models.

Langmuir Parameters					Freundlic	Freundlich Parameters				
Biochar	Q_{max} (mg g ⁻¹)	K _L (L mg ⁻¹)	\mathbb{R}^2	χ^2	K_{F}	1/n	R^2	χ^2	$R_{\rm L}$
AC350	5.8	0.01	0.987		0.03	0.14	0.67	0.986	0.05	0.5-0.9
AC400	6.6	0.02	0.906		0.58	0.22	0.64	0.858	0.75	0.4-0.9
AC450	4.9	0.08	0.996		0.02	0.95	0.35	0.948	0.13	0.10-0.5
AC500	5.8	0.05	0.940		0.28	0.81	0.41	0.834	0.63	0.14-0.6
AC500	4.9	0.20	0.924		0.18	1.03	0.37	0.887	0.34	0.04-0.3
AC600	5.9	0.16	0.988		0.07	1.68	0.29	0.929	0.25	0.05-0.3
AC650	13.1	0.24	0.993		0.38	3.45	0.36	0.976	0.36	0.03-0.3
AC700	37.5	0.13	0.918		1.86	4.96	0.66	0.945	0.79	0.06-0.4
Darco-AC	15.7	6.46	0.950		0.428	8.23	0.31	0.830	1.56	0.001 - 0.01

This factor is used to determine whether the adsorption is favorable or not. Values on the interval $0 < R_L < 1$ indicate that the adsorption is favorable. A value $R_L > 1$ is unfavorable, $R_L = 0$ means adsorption is irreversible, and $R_L = 1$ means there is a linear relation [63]. In this

study $R_L < 1$ showing the favorability of the adsorption process.

To extend our understanding of biochar ability to adsorption PO_4^{3-} , we plotted surface area and pH with respect to the adsorption capacity (see Fig. 11). The results demonstrate an increase in the adsorption

Table 3 Overview of results reported in the literature for other adsorbents for H_2S and $PO_4{}^{3-}$ removal.

Biomass source	Preparation method	Properties	Observations	Ref.
H ₂ S removal				
Oil palm shell	Physically and Chemically Activated materials	Surface area: 1014–1062 m ² /g Adsorption capacity: 46–76 mg H ₂ S/g	Physisorption, chemisorption and H ₂ S oxidation are important	[5]
Black liquor	Produced in a fluidized bed at 450 °C, steam activation	Surface area: 60 m ² /g. Adsorption capacity: 70 mg g ⁻¹ (AC for comparison purposes: 19 mg H ₂ S/g)	Fluidized bed contribute to the production of a carbon with a high adsorption capacity	[19]
Perilla leaf, soybean stover, Korean Oak, Japanese Oak	Pyrolyzed at 700 °C in a muffle furnace	Surface area: between 270 and 470 m ² /g. Adsorption capacity: 5–19 mg H ₂ S/g.	The highest breakthrough capacities for H ₂ S were obtained for perilla biochar	[21]
Commercial activated carbons	All the carbons were KOH impregnated	Surface area: 619–777 m ² /g. Adsorption capacity: 50–210 mg H ₂ S/g	Both chemisorption and physical adsorption are important mechanisms	[23]
Sewage sludge	Fluidized bed in N ₂ atmosphere, (T between 400 and 950 °C)	Surface area: 41–181 m ² /g Adsorption capacity: 8.2–57.5 mg H ₂ S/g.	Adsorption depend on physisorption, chemisorption and H ₂ S oxidation	[24]
Anaerobic digested fiber	Pyrolysis and CO ₂ activation (T: 350–800 °C)	Surface area: 36–305 m ² /g Adsorption capacity: 21.9–51.2 mg H ₂ S/g	Both physisorption and chemisorption are important	This work
Phosphate removal		5 2.7 G		
Anaerobically digested sugar beet tailings	Pyrolysis at 600 °C in a N ₂ environment for 2 h.	Surface area: $336 \mathrm{m}^2/\mathrm{g}$ Adsorption capacity: $133 \mathrm{mg g}^{-1}$	Controlled by adsorption on MgO nanoparticles.	[20]
Coir pith	Pyrolysis at 700 °C and activated with ZnCl ₂	Adsorption capacity 5.1 mg PO ₄ ³⁻ /g.	Ion exchange and chemisorption important	[29]
Sugar beet tailings and peanut shells	MgO-biochar nanocomposites.	Surface area: 19–122 m ² /g Adsorption capacity: as high as 835 mg PO ₄ ³⁻ /g	Calcining increased the surface area of MgO flakes	[30]
Anaerobic digested fiber	Pyrolysis and ${\rm CO_2}$ activation between 350 $^{\circ}{\rm C}$ and 800 $^{\circ}{\rm C}$	Surface area 36–305 m ² /g Adsorption capacity: 4.9–37.4 mg PO ₄ ³⁻ /g.	Retention governed by the ash content, surface area and pH.	This work

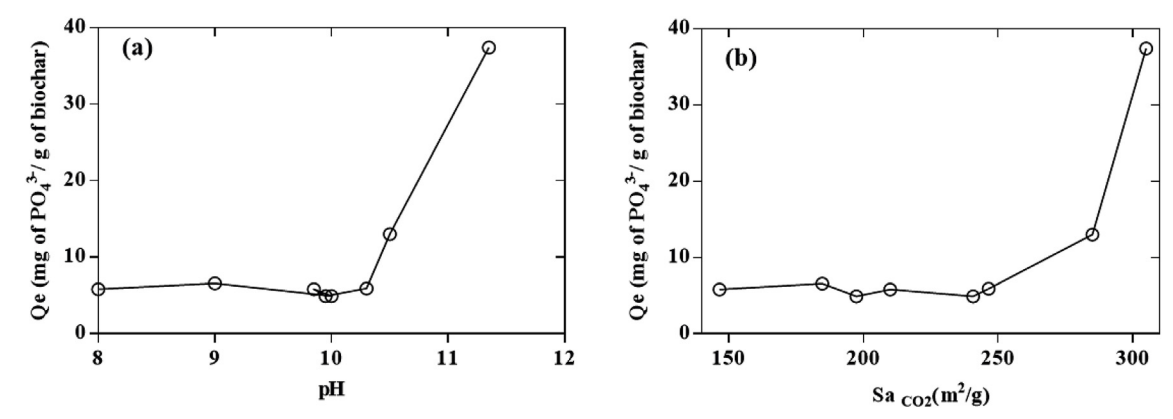


Fig. 11. (a) Relationship between pH and the maximum adsorption capacity, (b) Relationship between surface area and the maximum adsorption capacity.

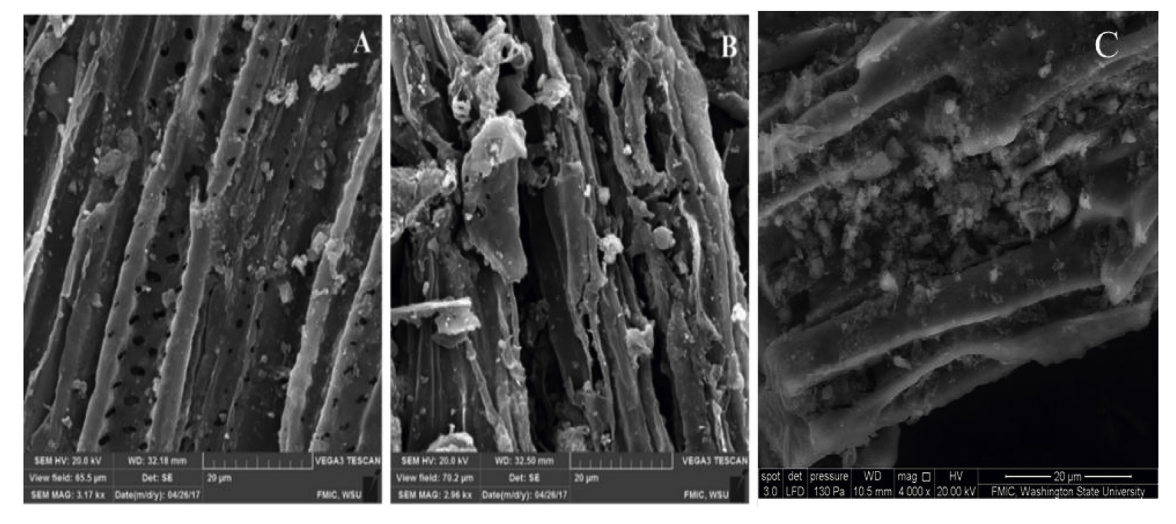


Fig. 12. SEM micrograph of (A) biochar before adsorption, (B) Biochar after H_2S adsorption, and (C) Biochar after $PO_4^{\ 3}$ adsorption.

capacity exponentially with respect to the surface area, and the pH. The fact that we were not able to find linear relations with a single intensive physico-chemical property suggest that the adsorption of PO_4^{3-} is a multistep process [64].

While the PO_4^{3-} sorption capacity is similar for lower temperature biochars (350–600 °C), for biochar produced at 650 and 700 °C the PO_4^{3-} sorption increases significantly, reaching a value of 37.4 mg PO_4^{3-} as a capacity of maximum of adsorption. This behavior is explained by the higher ash content in these biochars. When studies were done using biochar at 750 °C, the char completely adsorbed all the PO_4^{3-} in the aqueous phase (data not presented). This remarkable performance of biochar produced from AD fiber could be due to the presence of mineral content forming a carbon nanoparticle structure which leads to an increase in more actives sites to retain PO_4^{3-} . Similar work was done in previous studies, where calcium, magnesium and iron were doped on the surface of biochar that also performed well in PO_4^{3-} removal [28,32,64,65].

Fig. 12 presents SEM images providing evidence of structural changes after H_2S and $PO_4^{\ 3-}$ adsorption. The former (SEM after H_2S adsorption) shows an exfoliated structure due the formation of sulfuric acid; whereas the later (SEM after $PO_4^{\ 3-}$ adsorption) shows a structure attributed to possible precipitation of $PO_4^{\ 3-}$ on the surface of the biochar due to the mineral presence.

Table 3 summarizes the surface area and H_2S and $PO_4^{\ 3-}$ adsorption capacity of several carbonaceous adsorbents reported in the literature. Our product compares very well with other adsorbents developed for H_2S and $PO_4^{\ 3-}$ removal but clearly there are possibilities to improve its adsorption capacity. The main advantage of our product is that it is produced from a waste stream from the anaerobic digestion which could dramatically reduce its production cost and improve its feasibility.

4. Conclusion

The active biochar produced demonstrated the capacity to adsorb H₂S and PO₄³⁻. The production temperature of the biochar had a significant influence on the capacity of the resulting biochar towards H2S and PO₄³⁻ adsorption and retention. The ash content and adsorption in micropores are considered to be the driving forces for these processes. ICP-MS results show the high concentration of calcium, magnesium and iron, which has been demonstrated as the main components for the retention of H₂S and PO₄³⁻. This research shows the potential of AD fiber biochar as a remediation material. Therefore, this work concludes that the use of active biochar derived from AD fiber has capacity for H₂S removal from AD biogas and phosphates from the AD effluent. Also, utilizing the resulting nutrient-rich biochar as fertilizer will create social, economic and environmental benefits. Such holistic approach is needed to unleash the great potentials of thermochemical conversion, anaerobic digestion, and biochar carbon sequestration. Further research is required to standardize the design rules of biochar, which govern feedstock selection and carbonization conditions, leading to desired characteristics for specific pollutant removal capabilities.

Acknowledgements

Dr. Garcia-Perez is very thankful for the financial support provided by the US National Science Foundation (CBET-1703052). This activity was funded, in part, with an Applied BioEnergy Research Program Internal Competitive Grant from the Agricultural Research Center at Washington State University, College of Agricultural, Human, and Natural. The financial contribution of the Washington State department of Ecology Waste to Fuel program is greatly appreciated. This project was also partially funded by the USDA/NIFA through Hatch Projects # 1014753.

References

- S. Uludag-Demirer, G.N. Demirer, C. Frear, S. Chen, Anaerobic digestion of dairy manure with enhanced ammonia removal, J. Environ. Manag. 86 (2008) 193.
- [2] A.C. Wilkie, Anaerobic digestion: biology and benefits, Dairy Manure Management: Treatment, Handling, and Community Relations, 2005, p. 63.
- [3] R.E. Speece, Anaerobic Biotechnology for Industrial Wastewaters, (1996) Anaerobic biotechnology for industrial wastewaters.
- [4] J.B. Holm-Nielsen, T. Al Seadi, P. Oleskowicz-Popiel, The future of anaerobic digestion and biogas utilization, Bioresour. Technol. 100 (2009) 5478.
- [5] J. Guo, Y. Luo, A.C. Lua, R-a Chi, Y-I Chen, X-t Bao, et al., Adsorption of hydrogen sulphide (H 2 S) by activated carbons derived from oil-palm shell, Carbon 45 (2007) 330.
- [6] P. Kaparaju, J. Rintala, Mitigation of greenhouse gas emissions by adopting anaerobic digestion technology on dairy, sow and pig farms in Finland, Renew. Energy 36 (2011) 31.
- [7] P. Hobson, N. Feilden, Production and use of biogas in agriculture, Prog. Energy Combust. Sci. 8 (1982) 135.
- [8] J. Rico, H. García, C. Rico, I. Tejero, Characterisation of solid and liquid fractions of dairy manure with regard to their component distribution and methane production, Bioresour. Technol. 98 (2007) 971.
- [9] K. Güngör, K. Karthikeyan, Phosphorus forms and extractability in dairy manure: a case study for Wisconsin on-farm anaerobic digesters, Bioresour. Technol. 99 (2008) 425.
- [10] C. MacConnell, H. Collins, Utilization of re-processed anaerobically digested fiber from dairy manure as a container media substrate, International Symposium on Growing Media, 819 2007, p. 279 2007.
- [11] M.R. Pelaez-Samaniego, R.L. Hummel, W. Liao, J. Ma, J. Jensen, C. Kruger, et al., Approaches for adding value to anaerobically digested dairy fiber, Renew. Sustain. Energy Rev. 72 (2017) 254.
- [12] J.D. Streubel, H.P. Collins, J.M. Tarara, R.L. Cochran, Biochar produced from anaerobically digested fiber reduces phosphorus in dairy lagoons, J. Environ. Qual. 41 (2012) 1166.
- [13] Y. Yao, B. Gao, M. Inyang, A.R. Zimmerman, X. Cao, P. Pullammanappallil, et al., Biochar derived from anaerobically digested sugar beet tailings: characterization and phosphate removal potential, Bioresour. Technol. 102 (2011) 6273.
- [14] G. Soreanu, M. Béland, P. Falletta, K. Edmonson, P. Seto, Laboratory pilot scale study for H2S removal from biogas in an anoxic biotrickling filter, Water Sci. Technol. 57 (2008) 201.
- [15] R. Kleerebezem, R. Mendezà, Autotrophic denitrification for combined hydrogen sulfide removal from biogas and post-denitrification, Water Sci. Technol. 45 (2002) 349
- [16] S. Nishimura, M. Yoda, Removal of hydrogen sulfide from an anaerobic biogas using a bio-scrubber, Water Sci. Technol. 36 (1997) 349.
- [17] Q. Zhao, E. Leonhardt, C. MacConnell, C. Frear, S. Chen, Purification Technologies for Biogas Generated by Anaerobic Digestion, Compressed Biomethane, CSANR, 2010.
- [18] C. Zhang, C. Lai, G. Zeng, D. Huang, C. Yang, Y. Wang, et al., Efficacy of carbonaceous nanocomposites for sorbing ionizable antibiotic sulfamethazine from aqueous solution. Water Res. 95 (2016) 103.
- [19] Y. Sun, J.P. Zhang, C. Wen, L. Zhang, An enhanced approach for biochar preparation using fluidized bed and its application for H 2 S removal, Chem. Eng. Process: Process Intensification 104 (2016) 1.
- [20] Y. Yao, B. Gao, M. Inyang, A.R. Zimmerman, X. Cao, P. Pullammanappallil, et al., Removal of phosphate from aqueous solution by biochar derived from anaerobically digested sugar beet tailings, J. Hazard Mater. 190 (2011) 501.
- [21] S. Sethupathi, M. Zhang, A.U. Rajapaksha, S.R. Lee, N. Mohamad Nor, A.R. Mohamed, et al., Biochars as potential adsorbers of CH4, CO2 and H2S, Sustainability 9 (2017) 121.
- [22] A. Bagreev, T.J. Bandosz, A role of sodium hydroxide in the process of hydrogen sulfide adsorption/oxidation on caustic-impregnated activated carbons, Ind. Eng. Chem. Res. 41 (2002) 672.
- [23] R. Yan, D.T. Liang, L. Tsen, J.H. Tay, Kinetics and mechanisms of H2S adsoprtion by alkaline activated carbon, Environ. Sci. Technol. 36 (2002) 4460–4466.
- [24] A. Bagreev, S. Bashkova, D.C. Locke, T.J. Bandosz, Sewage sludge-derived materials as efficient adsorbents for removal of hydrogen sulfide, Environ. Sci. Technol. 35 (2001) 1537.
- [25] A. Bagreev, T.J. Bandosz, On the mechanism of hydrogen sulfide removal from moist air on catalytic carbonaceous adsorbents, Ind. Eng. Chem. Res. 44 (2005) 530.
- [26] A. White, D.W. Kirk, J.W. Graydon, Analysis of small-scale biogas utilization systems on Ontario cattle farms, Renew. Energy 36 (2011) 1019–1025.
- [27] S. Pipatmanomai, S. Kaewluan, T. Vitidsant, Economic assessment of biogas to electricity generation system with H2S removal by activated carbon in small pig farm, Appl. Energy 86 (2009) 669–674.
- [28] Y. Yao, B. Gao, J. Chen, M. Zhang, M. Inyang, Y. Li, et al., Engineered carbon (biochar) prepared by direct pyrolysis of Mg-accumulated tomato tissues: characterization and phosphate removal potential, Bioresour. Technol. 138 (2013) 8.
- [29] B.K. Biswas, K. Inoue, K.N. Ghimire, H. Harada, K. Ohto, H. Kawakita, Removal and recovery of phosphorus from water by means of adsorption onto orange waste gel loaded with zirconium, Bioresour. Technol. 99 (2008) 8685.
- [30] P. Kumar, S. Sudha, S. Chand, V.C. Srivastava, Phosphate removal from aqueous solution using coir-pith activated carbon, Separ. Sci. Technol. 45 (2010) 1463.
- [31] C. Namasivayam, D. Sangeetha, Equilibrium and kinetic studies of adsorption of phosphate onto ZnCl 2 activated coir pith carbon, J. Colloid Interface Sci. 280

- (2004) 359
- [32] M. Zhang, B. Gao, Y. Yao, Y. Xue, M. Inyang, Synthesis of porous MgO-biochar nanocomposites for removal of phosphate and nitrate from aqueous solutions, Chem. Eng. J. 210 (2012) 26.
- [33] C. Teater, Z. Yue, J. MacLellan, Y. Liu, W. Liao, Assessing solid digestate from anaerobic digestion as feedstock for ethanol production, Bioresour. Technol. 102 (2011) 1856
- [34] J.D. Streubel, Biochar: its Characterization and Utility for Recovering Phosphorus from Anaerobic Digested Dairy Effluent, Washington State University, 2011.
- [35] G. Shang, G. Shen, L. Liu, Q. Chen, Z. Xu, Kinetics and mechanisms of hydrogen sulfide adsorption by biochars, Bioresour. Technol. 133 (2013) 495.
- [36] M. Latos, P. Karageorgos, N. Kalogerakis, M. Lazaridis, Dispersion of odorous gaseous compounds emitted from wastewater treatment plants, Water, Air, Soil Pollut. 215 (2011) 667.
- [37] E.Y. Lee, N.Y. Lee, K.-S. Cho, H.W. Ryu, Removal of hydrogen sulfide by sulfateresistant Acidithiobacillus thiooxidans AZ11, J. Biosci. Bioeng. 101 (2006) 309.
- [38] G.P. Ferraz, C. Frear, M.R. Pelaez-Samaniego, K. Englund, M. Garcia-Perez, Hot water extraction of anaerobic digested dairy fiber for wood plastic composite manufacturing, BioResources 11 (2016) 8139.
- [39] D. Arenas-Lago, F. Vega, L. Silva, M. Andrade, Soil interaction and fractionation of added cadmium in some Galician soils, Microchem. J. 110 (2013) 681.
- [40] M.M. Dubinin, E. Zaverina, L. Radushkevich, Sorption and structure of active carbons. I. Adsorption of organic vapors, Zh. Fiz. Khim. 21 (1947) 151.
- [41] M.M. Dubinin, L. Radushkevich, Equation of the characteristic curve of activated charcoal, Chem Zentr, 1 1947, p. 875.
- [42] B. Pecha, P. Arauzo, M. Garcia-Perez, Impact of combined acid washing and acid impregnation on the pyrolysis of Douglas fir wood, J. Anal. Appl. Pyrol. 114 (2015) 127
- [43] C. Hach, Molybdovanadate with Acid Persulfate Digestion Method1 Method 10127 1.0 to 100.0 mg/L PO43– (HR) vol. 9, (2014).
- [44] A. Dada, A. Olalekan, A. Olatunya, O. Dada, Langmuir, Freundlich, Temkin and Dubinin–Radushkevich isotherms studies of equilibrium sorption of Zn2+ unto phosphoric acid modified rice husk, IOSR J. Appl. Chem. 3 (2012) 38.
- [45] J.P. Sheets, L. Yang, X. Ge, Z. Wang, Y. Li, Beyond land application: emerging technologies for the treatment and reuse of anaerobically digested agricultural and food waste, Waste Manag. 44 (2015) 94.
- [46] M.W. Smith, B. Pecha, G. Helms, L. Scudiero, M. Garcia-Perez, Chemical and morphological evaluation of chars produced from primary biomass constituents: cellulose, xylan, and lignin, Biomass Bioenergy 104 (2017) 17.
- [47] W. Suliman, J.B. Harsh, N.I. Abu-Lail, A.-M. Fortuna, I. Dallmeyer, M. Garcia-Perez, Influence of feedstock source and pyrolysis temperature on biochar bulk and surface properties. Biomass Bioenergy 84 (2016) 37.
- [48] G. Shang, Q. Li, L. Liu, P. Chen, X. Huang, Adsorption of hydrogen sulfide by biochars derived from pyrolysis of different agricultural/forestry wastes, J. Air Waste Manag. Assoc. 66 (2016) 8.
- [49] N. Sadhwani, S. Adhikari, M.R. Eden, Biomass gasification using carbon dioxide: effect of temperature, CO2/C ratio, and the study of reactions influencing the

- process, Ind. Eng. Chem. Res. 55 (2016) 2883.
- [50] F. Yang, C. Chi, C. Wang, Y. Wang, Y. Li, High graphite N content in nitrogen-doped graphene as an efficient metal-free catalyst for reduction of nitroarenes in water, Green Chem. 18 (2016) 4254.
- [51] J. Rivera-Utrilla, M. Sánchez-Polo, Ozonation of naphthalenesulphonic acid in the aqueous phase in the presence of basic activated carbons, Langmuir 20 (2004) 0217
- [52] M. Sánchez-Polo, U. Von Gunten, J. Rivera-Utrilla, Efficiency of activated carbon to transform ozone into OH radicals: influence of operational parameters, Water Res. 39 (2005) 3189.
- [53] B. Chen, D. Zhou, L. Zhu, Transitional adsorption and partition of nonpolar and polar aromatic contaminants by biochars of pine needles with different pyrolytic temperatures, Environ. Sci. Technol. 42 (2008) 5137.
- [54] M. Keiluweit, P.S. Nico, M.G. Johnson, M. Kleber, Dynamic molecular structure of plant biomass-derived black carbon (biochar), Environ. Sci. Technol. 44 (2010) 1247
- [55] Z. Wang, H. Zheng, Y. Luo, X. Deng, S. Herbert, B. Xing, Characterization and influence of biochars on nitrous oxide emission from agricultural soil, Environ. Pollut. 174 (2013) 289.
- [56] Y. Xu, B. Chen, Investigation of thermodynamic parameters in the pyrolysis conversion of biomass and manure to biochars using thermogravimetric analysis, Bioresour. Technol. 146 (2013) 485.
- [57] L. Jiang, S. Hu, Y. Wang, S. Su, L. Sun, B. Xu, et al., Catalytic effects of inherent alkali and alkaline earth metallic species on steam gasification of biomass, Int. J. Hydrogen Energy 40 (2015) 15460.
- [58] S. Boppart, Impregnated carbons for the adsorption of H~ 2S and mercaptans, Preprints of Papers-American Chemical Society division fuel chemistry, 41 1996, p. 389.
- [59] A. Ansari, A. Bagreev, T.J. Bandosz, Effect of adsorbent composition on H2S removal on sewage sludge-based materials enriched with carbonaceous phase, Carbon 43 (2005) 1039.
- [60] F. Adib, A. Bagreev, T.J. Bandosz, Adsorption/oxidation of hydrogen sulfide on nitrogen-containing activated carbons, Langmuir 16 (2000) 1980.
- [61] K. Foo, B. Hameed, Insights into the modeling of adsorption isotherm systems, Chem. Eng. J. 156 (2010) 2.
- [62] K.R. Hall, L.C. Eagleton, A. Acrivos, T. Vermeulen, Pore-and solid-diffusion kinetics in fixed-bed adsorption under constant-pattern conditions, Ind. Eng. Chem. Fundam. 5 (1966) 212.
- [63] H.N. Tran, S.-J. You, H.-P. Chao, Effect of pyrolysis temperatures and times on the adsorption of cadmium onto orange peel derived biochar, Waste Manag. Res. 34 (2016) 129.
- [64] Y. Yao, B. Gao, J. Chen, L. Yang, Engineered biochar reclaiming phosphate from aqueous solutions: mechanisms and potential application as a slow-release fertilizer, Environ. Sci. Technol. 47 (2013) 8700.
- [65] M. Zhang, B. Gao, Removal of arsenic, methylene blue, and phosphate by biochar/ AlOOH nanocomposite, Chem. Eng. J. 226 (2013) 286.